Int J Thermophys (2010) 31:2246–2263
DOI 10.1007/s10765-010-0866-x

A Study on Thermal Properties and $\alpha(hcp) \rightarrow \beta(bcc)$ Phase Transformation Energetics in Ti–5 mass% Ta–1.8 mass% Nb Alloy Using Inverse Drop Calorimetry

Madhusmita Behera · S. Raju · B. Jeyaganesh · R. Mythili · S. Saroja

Received: 19 May 2010 / Accepted: 27 October 2010 / Published online: 19 November 2010

Abstract Accurate measurements of enthalpy increment ($H_T - H_{298.15}$) values have been made on a Ti–5 mass% Ta–1.8 mass% Nb alloy using the inverse drop calorimetry technique in the temperature range from 463 K to 1457 K. The measured enthalpy increment values show a steady increase with temperature in both α-*hcp* and β-*bcc* solid solution regions. It is found that both the onset as well the completion of the $\alpha \rightarrow \beta$ phase change are demonstrated by a marked deviation of the enthalpy increment behavior from the otherwise smooth variation encountered in the respective low-temperature α- and high-temperature β-phase domains. The transformation start (T_s) and finish (T_f) temperatures of the $\alpha \rightarrow \beta$ phase change are found to be (1072 ± 10) K and (1156 ± 10) K, respectively. In the actual $\alpha \rightarrow \beta$ phase transformation region, the variation of the enthalpy with the progress of transformation is found to follow a sigmoidal shape which is in line with the diffusive nature of the phase transformation. An estimation of the total enthalpy change associated with the $\alpha \rightarrow \beta$ phase transformation ($\Delta^\circ H_{tr}$) has been made by assuming a simple diffusion limited kinetic model for the phase change. The net enthalpy change for the $\alpha \rightarrow \beta$ transformation is found to be 76 J · g^{-1}. The measured temperature variation of the enthalpy increment in both α- and β-phase regimes are fitted to simple analytical functional forms to obtain temperature-dependent estimates of the specific heat, C_P. The total specific heat change associated with the $\alpha \rightarrow \beta$ phase transformation $\Delta^\circ C_P^{\alpha \rightarrow \beta}$ is estimated to be 904 J · kg^{-1} · K^{-1}.

Madhusmita Behera—Senior Research Fellow, Homi Bhabha National Institute at IGCAR.

M. Behera · S. Raju (✉) · B. Jeyaganesh · R. Mythili · S. Saroja
Physical Metallurgy Division, Metallurgy and Materials Group,
Indira Gandhi Centre for Atomic Research, Kalpakkam 603102, India
e-mail: sraju@igcar.gov.in

Keywords Calorimetry · Enthalpy · Phase transformation · Specific heat · Thermodynamic properties · Titanium alloy

1 Introduction

It is rather well known that commercial titanium and titanium-based alloys find extensive applications in many diverse areas ranging from aerospace, chemical, biotechnology, and human prosthetic replacements, to name a few [1,2]. A somewhat recent addition to this growing list is the Ti–5 mass% Ta–1.8 mass% Nb alloy that is developed for nuclear fuel reprocessing applications, where a high level of corrosion resistance to boiling nitric acid is required [3,4]. This Ti–5 mass% Ta–1.8 mass% Nb alloy is basically an $\alpha(hcp)$-phase alloy, although the presence of $\beta(bcc)$-stabilizers such as niobium, tantalum, and some residual iron of about 7 mass% in total contributes to the presence of about 4 vol% to 5 vol% of the β-phase in the room temperature microstructure [5,6]. Despite the fact that a fair amount of microstructure-property characterization studies of this new $\alpha + \beta$ alloy has been carried out in the authors' laboratory [4–8], a detailed investigation of the thermodynamics and kinetic aspects of the phase stability and phase transformation is rather due. In the present study, we attempt to fill this gap partially by performing accurate drop calorimetry measurements on well-annealed homogeneous samples of the Ti–5 mass% Ta–1.8 mass% Nb alloy. The temperature range of investigation is from 463 K to 1457 K, which includes the $\alpha \rightarrow \beta$ phase transformation domain as well. The motivation behind this work is to obtain reliable estimates of the enthalpy and specific heat over regions of stability of both α- and β-phases, besides probing calorimetrically the nature of the $\alpha \rightarrow \beta$ transformation. The experimental details are given in the ensuing section.

2 Experimental Details

2.1 Basic Characterization of the Alloy

The alloy used in this study is prepared by vacuum arc melting in the Nuclear Fuel Complex, Hyderabad, India. The chemical composition of the alloy as determined by wet chemical analysis is listed in Table 1. The primary ingot after suitable thermomechanical processing is received in the form of rods. This alloy has been subsequently stress relieved by holding at 973 K for about 5 h. The basic microstructural characterization has been carried out using optical microscopy (Leica MeF4A) and scanning electron microscopy (Philips XL-30). The samples for metallography are prepared by conventional mechanical polishing followed by etching with Kroll's reagent (2 mL HF + 8 mL HNO_3 + 90 mL H_2O). Phase identification has been carried out using the INEL® X-ray diffraction system employing Cu-K_α radiation in the 2θ range spanning from 20° to 90°. Pure Silicon powder (99.99 %) supplied by NPL, India has been employed as the calibration standard.

Table 1 Chemical composition of the alloy as determined by wet chemical analysis

Element	Ta	Nb	Fe	O	N	H	C	Ti
Concentration	4.39[a]	1.85[a]	263[b]	500[b]	47[b]	9[b]	125[b]	Balance

[a] Values in mass%
[b] Values in ppm by mass

2.2 Drop Calorimetry Studies

The inverse drop calorimetry studies are performed with a *Setaram multi HTC* 96® high-temperature calorimeter. The temperature and heat flux calibration of the instrument has been carried out with the melting point of pure Al and pure α-Al_2O_3 pellets supplied by *Setaram* respectively. Samples for calorimetry are taken in the form of small pieces with an average mass in the range (30 ± 0.1) mg to (60 ± 0.1) mg. These are cleaned with alcohol and dried prior to the experiment. Samples are loaded into the individual slots of the specimen holder provided at the top assembly of the calorimeter setup. The sample holder is kept at the reference temperature (room temperature). The furnace and experimental chambers are alternately evacuated and purged with high purity argon gas before the commencement of each experimental run. Subsequently, a steady argon flow of about $50\,\mathrm{mL} \cdot \mathrm{min}^{-1}$ is maintained throughout the experiment. The drop bed is made up of a small alumina crucible of capacity $6.25\,\mathrm{cm}^3$ filled up to two third of its total capacity with high pure alumina powder supplied by *Setaram.* This alumina bed is located at the bottom end of the long ceramic tube, which is heated by the surrounding graphite furnace. The temperatures of the furnace and sample are measured independently by a Pt/Pt–Rh thermocouple. The furnace is heated to the predetermined temperature at the rate of $5\,\mathrm{K} \cdot \mathrm{min}^{-1}$. When the temperature of the alumina bed has reached the preset value and remained constant to within about ± 0.2 K (which took about 6 h to 7 h), the samples are dropped one by one from their respective slots into the hot isothermal alumina bed through the guiding alumina tube. In order to ensure the attainment of complete thermal equilibrium of the bed after each successive drop experiment, a time interval of about 15 min to 20 min is allowed to elapse between successive drops. The experimental schedule is designed in such a manner that the dropping of each Ti–Ta–Nb sample is followed immediately (after allowing for the statutory waiting period required for achieving thermal equilibrium of the bed) by that of a reference α-Al_2O_3 pellet under nearly identical conditions. This ensures that the basic drop calorimetry signal, namely, the change in bed temperature (ΔT) with time (t) recorded during the thermal equilibration of the bed after dropping of the alloy, is reliably calibrated in terms of a similar datum collected with the reference sample or calibrant whose enthalpy increment at the set temperature is known *a priori*. Assuming negligible heat loss due to radiation, the measured total heat flux Q_s transacted in the course of drop experiment of the alloy may be written as follows [9]:

$$Q_s = C(T) \times (m_s/M_s) \times (H_T - H_{298})_s \tag{1}$$

In Eq. 1, m_s is the mass of the alloy sample, M_s is the average molar mass of the alloy, $H_T - H_{298}$ is the enthalpy increment at T with respect to the reference temperature, 298 K, and C is the empirical temperature-dependent calorimeter constant. The parameter $C(T)$ can be evaluated from a knowledge of the heat flux change measured in the drop experiment of the reference α-Al_2O_3 sample and from a knowledge of its assessed enthalpy increment data [10]. Thus, for reference we may write an equation similar to Eq. 1;

$$Q_R = C(T) \times (m_R/M_R) \times (H_T - H_{298})_R \tag{2}$$

Here, m_R and M_R stand, respectively, for the actual and molar mass of the reference. $(H_T - H_{298})_R$ is the enthalpy increment of the reference sample. Once $C(T)$ is estimated as a function of temperature from Eq. 2, it is a straightforward task to calculate the enthalpy increment of the alloy sample, using Eq. 1. In the present study, drop experiments are conducted in the temperature range from 463 K to 1457 K using fresh individual samples for each drop. The temperature interval between each successive drop is chosen as 25 K. The drop experiments are conducted in three separate runs or schedules. In each of these schedules the isothermal drop experiment is performed at successively higher temperatures, with approximately 25 K as the temperature step. Further, in each of these runs, different starting temperatures, say from 463 K, 488 K, and 523 K are adopted so that in the temperature interval 463 K to 1457 K, quite a good number of data points are gathered. In the β-phase domain, some additional experiments are also carried out with a smaller than 25 K temperature interval, to get improved statistics in the high-temperature region, where the data scatter is expected to be relatively high. In addition, metallographic characterization of selected samples that are dropped from the transformation temperature zone have also been carried out to qualitatively assess the extent of the phase transformation as a function of temperature. An estimate of the volume fraction of the β-phase in these samples is carried out using the image analysis software ImageJ® (available on http://rsb.info.nih.gov/ij/index.html). These experimental results are described in the following section.

3 Results

3.1 Initial Characterization of the Alloy

The microstructure of this alloy is shown in Fig. 1. It is observed that the microstructure consists of well-defined equiaxed α-grains, characteristic of an annealed state. The XRD pattern taken at room temperature is shown in Fig. 2. The presence of the major α-*hcp* phase is clearly evident from the X-ray profile. Based on chemical composition (Table 1), the present alloy is expected to be an $\alpha+\beta$ two-phase alloy. However, optical microscopy observations, and especially the XRD pattern, did not reveal unequivocally the diffraction lines that are characteristic of the *bcc*-phase. Possible reasons for this could be the strong overlap of the major β-phase reflections with the matrix α-lines and further, the volume fraction of β being small to make a distinct registry of its own weak reflections [11]. The presence of a small amount of the β-phase in this

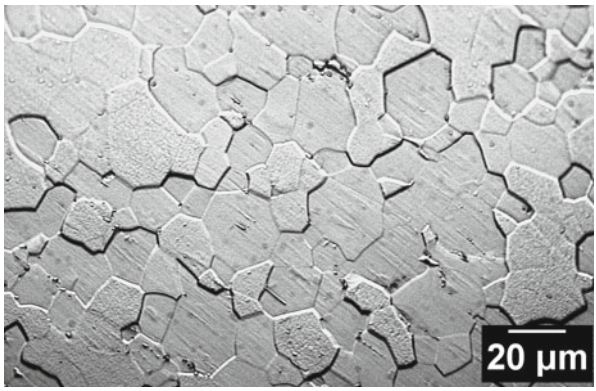

Fig. 1 Optical micrograph of the Ti–5 mass% Ta–1.8 mass% Nb alloy annealed at 973 K/5 h showing equiaxed grains

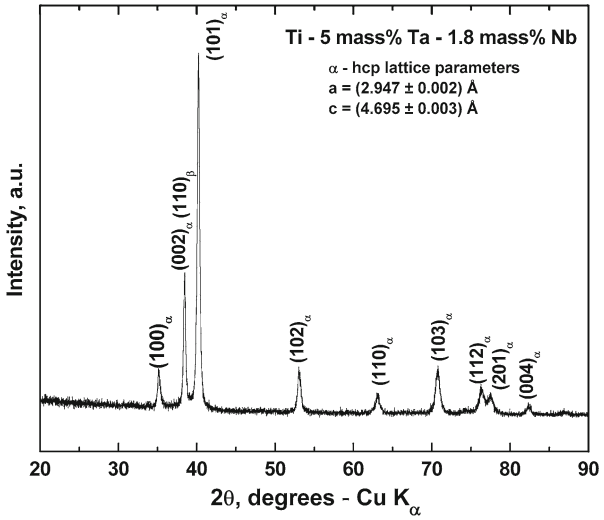

Fig. 2 Room temperature XRD pattern of the Ti–5 mass% Ta–1.8 mass% Nb alloy showing the presence of α-phase peaks

alloy has been confirmed based on microstructural evidence obtained using electron microscopy [5]. In Table 2, the X-ray diffraction results are summarized and the calculated lattice parameter values for the α-phase are also listed. Since, to the best of our knowledge, no prior structural characterization of this alloy has been reported in the literature, a comparison of the lattice parameter of this alloy with reported values for other related Ti-based alloys has also been made in Table 3 [12–17]. It is readily observed that there is a close agreement between the lattice parameter values of the present alloy with reported ones at related compositions.

Table 2 Details of X-ray diffraction data on Ti–5 mass% Ta–1.8 mass% Nb alloy

S. No.	2θ (°)	Normalized intensity	(hkil) value	Lattice parameter (Å)
1	35.121	13.9	$(10.0)_\alpha$	$a = (2.947 \pm 0.002)$ Å
2	38.481	40.1	$(00.2)_\alpha$	$c = (4.695 \pm 0.003)$ Å
			$(110)_\beta$	$c/a = 1.593$
3	40.233	100	$(10.1)_\alpha$	
4	53.025	14.4	$(10.2)_\alpha$	
5	62.985	7.3	$(11.0)_\alpha$	
6	70.773	14.7	$(10.3)_\alpha$	
7	76.293	9.6	$(11.2)_\alpha$	
8	77.361	6.9	$(20.1)_\alpha$	
9	82.329	4.7	$(00.4)_\alpha$	

Table 3 Lattice parameters of Ti–5 mass% Ta–1.8 mass% Nb alloy and a few other titanium alloys having α (*hcp*), α' (*hcp*-martensite), and α'' (orthorhombic-martensite) phases

Alloy	Lattice parameter (Å)		c/a	Reference
	a	c		
Ti	2.9503	4.6810	1.587	[12]
Ti–5 mass% Ta–1.8 mass% Nb	2.947 ± 0.002	4.695 ± 0.003	1.593	Present work
Ti–6 mass% Al–4 mass% V	2.938	4.684	1.594	[13]
Ti–6 mass% Al–2 mass% Sn–4 mass% Zr–2 mass% Mo–0.08 mass%	2.942	4.698	1.597	[13]
Ti–4 mass% Nb–4 mass% Zr	2.964	4.697	1.584	[14]
Ti–2 mass% Mo	2.943	4.681	1.590	[15]
Ti–4 mass% Mo	2.945	4.676	1.588	[15]
VT14	2.92	4.68	1.602	[16]
α''-Orthorhombic phase				
Ti–25.5 mass% Nb	$a = 3.11$ Å		$b/a = 1.581$	[17]
	$b = 4.92$ Å		$c/a = 1.491$	
	$c = 4.64$ Å			

Data for the latter alloys are taken from Refs. [12–17]

3.2 Enthalpy Increment Variation with Temperature

Figure 3 shows the temperature variation of the enthalpy increment $(H_T - H_{298})$ measured in two typical experimental runs. In each of these runs, the isothermal drop experiment is performed at successively higher temperatures with a temperature interval of about 25 K. It is observed from Fig. 3 that the enthalpy increment $(H_T - H_{298})$ for the low-temperature α-phase increases steadily in a non-linear fashion

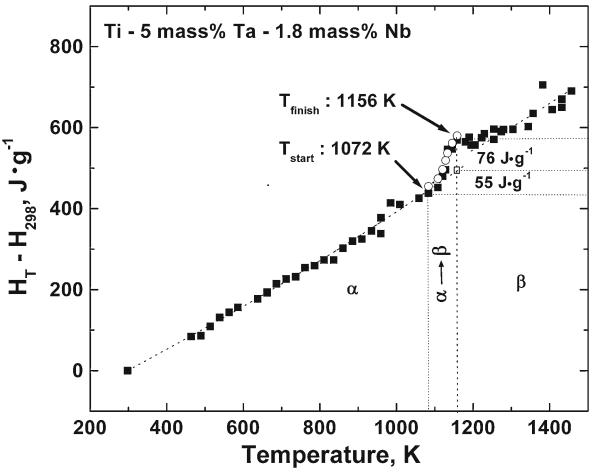

Fig. 3 Variation of enthalpy increment with temperature for Ti–5 mass% Ta–1.8 mass% Nb alloy

with
temperature up to about 1072 K. At this temperature there is a clear change in the enthalpy variation behavior indicating the possible commencement of the $\alpha \rightarrow \beta$ phase transformation [14]. In the $\alpha \rightarrow \beta$ transformation region, the enthalpy increment values show a steeply rising character with temperature. This trend persists up till about 1156 K and, subsequent to which, another marked change in the enthalpy variation has been observed. This second inflection temperature is taken to mark the approximate completion (T_f) of the β-phase formation. In the β-phase regime, the enthalpy again shows a continuous, non-linear increase with temperature.

3.3 Microstructural Changes During $\alpha \rightarrow \beta$ Transformation

Although the presence of distinct inflections in the enthalpy curve (Fig. 3) clearly attested to the occurrence of the $\alpha \rightarrow \beta$-phase change, it was also confirmed by an independent observation of the microstructural evolution at select temperatures in the transformation zone. This microstructural observation is carried out on samples that are dropped from the $\alpha \rightarrow \beta$ transformation temperature domain. The choice of the temperature is such that one sample each is drawn from just below the $\alpha \rightarrow \beta$ phase transformation start (T_s), in the actual $\alpha \rightarrow \beta$ transition region and just after the completion of the $\alpha \rightarrow \beta$ phase transformation. The microstructure of these alloy samples are collated in Fig. 4. It is observed from Fig. 4a that at 1060 K, a temperature that is a little lower than the actual $\alpha \rightarrow \beta$ phase transformation start temperature T_s, i.e., (*in the α-phase field*), a microstructure with equiaxed α-grains and fine inter- and intragranular β-precipitates is observed. This again confirms the deduction that at 1060 K, the matrix is predominantly α-grains and the β-phase is nucleated at the grain boundary. The relative amount of the β-phase fraction at this temperature is estimated to be about (3.73 $\pm$ 0.5) %. Figure 4b compares the EDS spectra collected from the

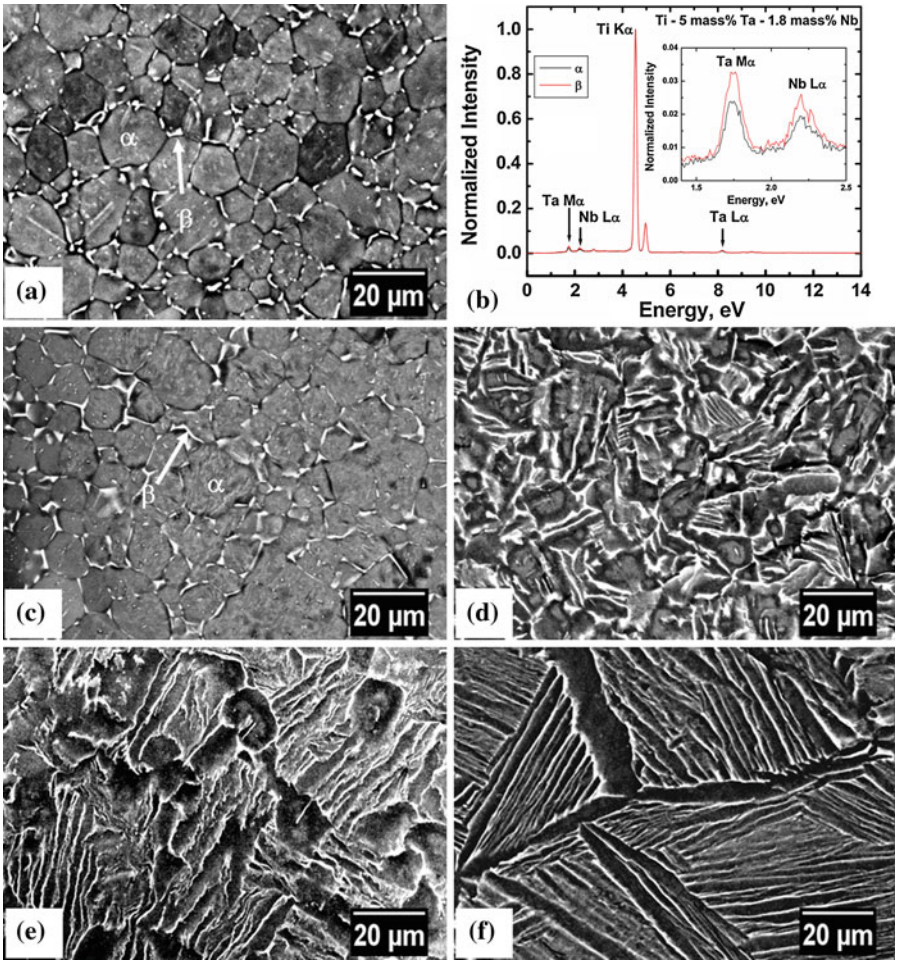

Fig. 4 (a) Back scattered electron image showing the primary α-phase at 1060 K, (b) EDS spectra corresponding to 1060 K obtained from α- and β-phases, and (c–f) back scattered electron images showing the variation in microstructural features with increasing temperature; (c) 1083 K, (d) 1120 K, (e) 1133 K, and (f) 1158 K

equiaxed α-grains and from the β-precipitates. It is clearly seen that the β-phase is slightly enriched in Ta and Nb content as compared to α-grains, a fact which suggests that certain solute repartitioning should have taken place during the course of formation of the β-phase. In Fig. 4c, the microstructure of the drop sample pertaining to a higher temperature, namely, 1083 K is shown. From this figure, a slight coarsening of the β-precipitates is noticed; the amount of β-phase at this temperature is estimated to be around $(6.56 \pm 1.3)\,\%$. At still higher temperatures, namely, 1120 K and 1133 K, the microstructure shown in Fig. 4d, e, respectively, consisted of a large amount of a transformed β fraction. In Fig. 4f, corresponding to a sample dropped from 1158 K, an almost fully transformed β structure is noticed and this indicates that the $\alpha \rightarrow \beta$ phase change is by and large complete at 1158 K. So judging from the microstructure point

of view as well, the temperature of 1158 K may be taken as the typical end point of the $\alpha \rightarrow \beta$ transformation. This temperature is in excellent agreement with the inflection point of 1156 K obtained from calorimetry data (Fig. 3). It is interesting to recall that this calorimetric estimate of the transformation finish temperature (T_f) is close to the β-transus temperature of 1143 K evaluated in our previous studies [11].

As a further remark, it may be said that in typical drop calorimetry studies, no matter how close the temperature interval is chosen, it is not possible to trace the enthalpy behavior with temperature in a continuous manner. We take into consideration this point and also in view of the fact that the first detectable evidence of the β-phase formation in drop calorimetry occurs only when the fraction transformed reaches a minimum threshold that is adequate to induce a measurable thermal effect. Thus, the true transformation start temperature is not detected in the drop calorimetry measurements. A similar limitation also exists for the metallographic detection of transformation onset as well. Despite these limitations, it is interesting to note that the drop calorimetry signature of the $\alpha \rightarrow \beta$ transformation domain is in fair accord with the microstructural evidence.

4 Discussion

4.1 Analytical Representation of Enthalpy Increment Data

The experimental enthalpy increment data in α-, $\alpha + \beta$, and β-phase regions are fitted to the following expressions and the corresponding specific heat (C_P) values are calculated from these expressions. The expression for the α-phase domain is chosen by fixing $\Delta^\circ H_{298.15} = 0$.

4.1.1 α-Phase: 463 K ≤ T ≤ 1072 K

$$\Delta^\circ H(\mathrm{J \cdot kg^{-1}}) = [H_T - H_{298.15}] = 399.64\,(T - 298.15) + 0.11\left(T^2 - 298.15^2\right) - 4825421.78\,(1/T - 1/298.15). \quad (3)$$

$$C_P(\mathrm{J \cdot kg^{-1} \cdot K^{-1}}) = \mathrm{d}\left(\Delta^\circ H\right)/\mathrm{d}T = 399.64 + 0.22T + 4825421.78T^{-2} \quad (4)$$

From Eq. 4, the specific heat C_P at 298.15 K is estimated to be 519 $\mathrm{J \cdot kg^{-1} \cdot K^{-1}}$. This value is in the same range as the ones reported for other related Ti-based alloys [18].

4.1.2 α → β Transformation Region: 1072 K ≤ T ≤ 1156 K

In the $\alpha + \beta$ two-phase domain the total enthalpy increment ($\Delta^\circ H_T$) at any temperature T is basically a sum of two independent contributions. Of these, the first comes from the weighted sum of individual enthalpy contributions from α- and β-phases. The other, termed as the phase transformation enthalpy ($\Delta^\circ H_{tr}$), arises

from the so-called latent heat associated with the $\alpha \rightarrow \beta$ phase transformation. Thus, to a first approximation, the total measured enthalpy increment ($\Delta^\circ H_T$) may be written as follows [19]:

$$\Delta^\circ H_T = \left[f_\alpha \Delta^\circ H_T^\alpha + f_\beta \Delta^\circ H_T^\beta \right] + f_\beta \Delta^\circ H_{\mathrm{tr}}. \tag{5}$$

where

$$f_\alpha(T) + f_\beta(T) = 1. \tag{6}$$

In the above equations, $f_\alpha(T)$ and $f_\beta(T)$ denote, respectively, the fraction of α- and β-phases present at temperature T; $\Delta^\circ H_T^\alpha$ is the enthalpy increment of the α-phase at temperature T, and $\Delta^\circ H_T^\beta$ is the enthalpy increment of the β-phase. The basis for the above approximation is the fact that in contrary to the phase change in a unary system, the $\alpha \rightarrow \beta$ phase transformation in an alloy occurs over a temperature range. Hence, at any temperature T in the transformation zone, namely, $T_\mathrm{s} \leq T \leq T_\mathrm{f}$, we have finite amounts of both α- and β-phases whose phase fractions f_α and f_β are, of course, functions of temperature. However, as a boundary condition, we also have that as $T \rightarrow T_\mathrm{f}$, $f_\alpha \rightarrow 0$ and $f_\beta \rightarrow 1$. Thus, at any intermediate temperature in the transformation zone $T_\mathrm{s} \leq T \leq T_\mathrm{f}$, we have a progressively increasing contribution to total enthalpy from the $\alpha \rightarrow \beta$ phase change.

It emerges therefore from the foregone discussion that an attempt to model the total enthalpy in the two-phase transformation zone in terms of Eq. 5 necessitates that $\Delta^\circ H_T^\alpha$, $\Delta^\circ H_T^\beta$, f_α, and f_β must be known as a function of temperature in the domain $T_\mathrm{s} \leq T \leq T_\mathrm{f}$. It is clear that both $\Delta^\circ H_T^\alpha$ and $\Delta^\circ H_T^\beta$ in the transition zone ought to be obtained as metastable extrapolations of their respective trends in their stable α- and β-phase stability domain. This is graphically illustrated in Fig. 3, wherein, the dotted line indicates the extrapolated enthalpy behavior of the α-phase in the $\alpha \rightarrow \beta$ transformation zone. This extrapolation is extended only up to T_f, the transformation finish temperature. Thus, in a physical sense, the indicated enthalpy difference of 55 $\mathrm{J \cdot g^{-1}}$ in Fig. 3 equals the differential quantity, $\Delta^\circ H_T^\alpha(T_\mathrm{f}) - \Delta^\circ H_T^\alpha(T_\mathrm{s})$; with the tacit understanding that $\Delta^\circ H_T^\alpha(T_\mathrm{f})$ is the extrapolated estimate of the α-phase enthalpy at T_f. Stated in other words, if one were to increase the temperature of the α-phase to T_f from T_s without allowing for it to transform to β, then this process would have entailed an enthalpy increase of the α-phase of 55 $\mathrm{J \cdot g^{-1}}$. Now in the second step, the $\alpha \rightarrow \beta$ transformation is allowed to take place at the fixed temperature $T = T_\mathrm{f}$; and this isothermal transformation step would result in an enthalpy change of 76 $\mathrm{J \cdot g^{-1}}$ (Fig. 3). This latter value corresponds to the total transformation enthalpy or the latent heat released during the process of the $\alpha \rightarrow \beta$ transformation. But it must be remembered that in the actual or continuous $\alpha \rightarrow \beta$ phase change, this net value of 76 $\mathrm{J \cdot g^{-1}}$ is distributed over the entire domain transformation domain $T_\mathrm{s} \leq T \leq T_\mathrm{f}$. At the transformation start temperature T_s, we have $f_\beta = 0$; $\Delta^\circ H_{\mathrm{tr}} = 0$, and at $T = T_\mathrm{f}$,

$\Delta^\circ H_{\rm tr} = 76\,{\rm J}\cdot{\rm g}^{-1}$. Thus, in the final analysis, the total enthalpy increment $\Delta^\circ H_T(T)$ in the $\alpha \rightarrow \beta$ transformation zone is given as

$$\Delta^\circ H_T/{\rm J}\cdot{\rm kg}^{-1} = [H_T - H_{298.15}] = \{399.64\,(T - 298.15) + 0.11\left(T^2 - 298.15^2\right) - 4825421.78\,(1/T - 1/298.15)\} + f_\beta \Delta^\circ H_{\rm tr.} \quad (7)$$

It is again worth reiterating the fact that the first term inside the braces on the right-hand side of Eq. 7 denotes the α-phase enthalpy which is extrapolated up to $T_{\rm f}$. The second term is the transformation component.

As for explaining the temperature dependence of the progress of the $\alpha \rightarrow \beta$ transformation, namely, $f_\beta(T)$, an empirical description of the diffusional phase transformation kinetics is invoked that goes by the name of the Kolmogorov–Johnson–Mehl–Avrami (KJMA) model. According to this model, $f_\beta(T)$ is given by the following expression [20]:

$$f_\beta(T) = 1 - \exp\{-k_0^n \exp\{(-nQ_{\rm eff}/RT)\}\,(R\,(T - T_{\rm s})^2/(\phi Q_{\rm eff}))^n\}. \quad (8)$$

Here, $Q_{\rm eff}$ represents the apparent activation energy for the *overall* transformation, n is an empirical transformation exponent, k_0 is the frequency factor, and R is the universal gas constant. It must be noted that Eq. 8 is a simple model for the isochronal transformation kinetics that is valid under certain conditions only [21,22]. In this sense, the parameter ϕ appearing in Eq. 8 should correspond ideally to slow rates of heating such that at each temperature T in the transformation zone, the equilibrium limit of $f_\beta(T)$ is realized. In the present set of drop calorimetry measurements, we allow for about 20 min to elapse between successive drops, and hence it is presumed that $f_\beta = f_\beta^{\rm eq}$ at each temperature interval in the transformation domain. Substituting Eq. 8 for $f_\beta(T)$ into Eq. 7, the experimental enthalpy data corresponding to the transformation temperature zone are fitted to obtain the following values for the fit parameters:

$$\begin{aligned} n &= 1.1; \\ Q_{\rm eff} &= 295\ {\rm kJ}\cdot{\rm mol}^{-1};\ \text{and} \\ k_0 &= 1.06\times 10^{13}{\rm s}^{-1}. \end{aligned}$$

The specific heat in the transformation zone can also be evaluated by taking the derivative of Eq. 7 with respect to T. The relevant expression for C_P is the following:

$$\Delta C_P^{\alpha\rightarrow\beta}/{\rm J}\cdot{\rm kg}^{-1}\cdot{\rm K}^{-1} = 399.64 + 0.22T + 4825421.78T^{-2} + f_\beta \Delta^\circ C_P + {\rm d}f_\beta/{\rm d}T\,(\Delta^\circ H_{\rm tr}). \quad (9)$$

Here, $\Delta^\circ C_P$ is the change in C_P associated with the $\alpha \rightarrow \beta$ phase transformation. Its value is estimated to be $(\Delta^\circ H_{\rm tr}/\Delta T) = 904\,{\rm J}\cdot{\rm kg}^{-1}\cdot{\rm K}^{-1}$.

4.1.3 Enthalpy Representation in β Region: 1156 K ≤ T ≤ 1457 K

In the β-phase region the enthalpy increment values are fitted to the following expression:

$$\Delta^\circ H_T(\mathrm{J}\cdot\mathrm{kg}^{-1}) = 225.15T + 0.15T^2 + 70534894.46T^{-1} \tag{10}$$

$$C_P = \mathrm{d}\left(\Delta^\circ H_T\right)/\mathrm{d}T = 225.15 + 0.3T - 70534894.46T^{-2} \tag{11}$$

The variation of C_P with temperature in the α-phase, in the phase transformation region, and in the β region are shown in Fig. 5. In Table 4, the experimental enthalpy increment data together with fit values are listed for select temperatures in the α- and β-phase regions. Since each experiment is conducted with fresh samples having different mass, the relevant information together with the measured value of the calorimeter signal given in $\mu\mathrm{V}\cdot\mathrm{s}\cdot\mathrm{g}^{-1}$ are also included in the tabulation. The corresponding C_P values obtained from the fit expressions are listed in Table 5.

4.1.4 Neumann–Kopp Approximation for C_P Evaluation

As not much data are available on thermal properties of advanced titanium alloys containing *bcc* transition elements, the measured specific heat values for the Ti–5 mass% Ta–1.8 mass% Nb alloy are compared with the reported values for a Ti–Nb–Zr alloy [14]. As may be seen in Fig. 5, the values for these two closely related alloys compare rather well. Besides, an attempt is also made to compare the present experimental values with the estimated results using the Neumann–Kopp (N–K) approximation which is given as [23]

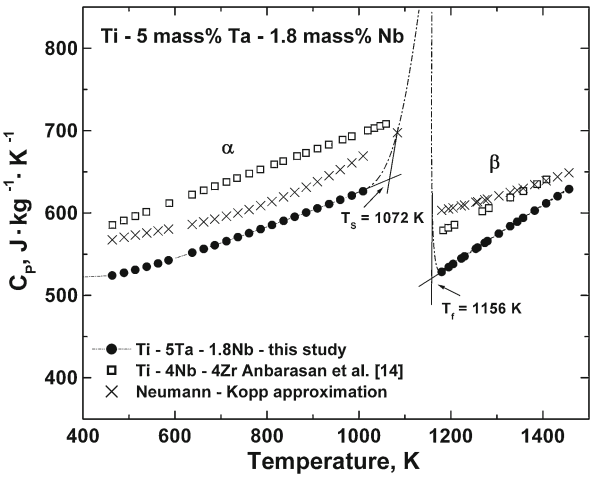

Fig. 5 Variation of specific heat C_P with temperature for Ti–5mass%Ta–1.8 mass% Nb alloy

Table 4 Experimental enthalpy increment data on Ti–5 mass% Ta–1.8 mass% Nb alloy at selected temperatures are listed together with fit values

T (K)	Mass (10^{-3} g)	Peak area ($10^3\ \mu V \cdot s \cdot g^{-1}$)	$\Delta^\circ H_T$ experimental ($J \cdot g^{-1}$)	$\Delta^\circ H_T$ Fit ($J \cdot g^{-1}$)	Difference (%)
α-Phase					
298			0 (set)	0	−−
464	29.1	9.38	84	86	−2
489	22.2	11.14	86	89	3
514	25.0	15.72	109	112	−3
539	29.5	21.75	132	126	5
563	29.3	26.24	144	139	4
586	22.9	30.70	156	151	3
638	26.6	36.63	177	179	−1
662	22.9	41.39	192	193	0
663	25.0	47.00	194	193	1
686	24.8	55.10	214	206	4
712	28.0	60.52	226	221	2
737	28.4	66.76	232	235	−1
761	26.3	74.30	254	249	2
786	21.2	82.70	259	263	−2
811	24.8	86.96	273	278	−2
836	28.6	90.65	273	293	−7
860	28.8	102.84	302	307	−1
885	22.6	111.82	319	322	−1
910	30.0	119.21	325	337	−4
935	34.9	128.42	345	352	−2
959	22.1	141.80	338	367	−8
985	27.6	164.79	414	383	8
1009	22.3	158.32	410	398	3
1059	22.4	180.76	426	429	−1
1084	24.3	232.88	438	445	−2
β-Phase					
1195	46.8	197.18	557	542	3
1205	53.7	212.18	557	548	2
1223	43.7	223.48	575	557	3
1230	48.6	235.61	585	561	4
1254	58.4	238.95	571	575	−1
1254	60.4	238.74	596	575	4
1258	54.3	230.87	617	577	7
1274	58.8	239.62	590	585	1
1280	58.9	244.92	595	589	1
1304	58.8	239.00	596	603	−1

Table 4 continued

T (K)	Mass (10^{-3} g)	Peak area (10^3 μV · s · g^{-1})	$\Delta^\circ H_T$ experimental (J · g^{-1})	$\Delta^\circ H_T$ Fit (J · g^{-1})	Difference (%)
1344	59.8	249.38	603	626	−4
1357	58.3	243.57	635	634	0
1382	61.3	238.99	705	649	8
1407	61.2	247.07	644	664	−3
1432	60.0	257.86	650	679	−4
1432	55.0	250.00	670	679	−1
1457	59.6	255.11	690	695	−1

Enthalpy values are rounded off to the nearest integer. The quality of fit is given by the percentage difference which is defined as $[\{\Delta^\circ H_T(\text{exp}) - \Delta^\circ H_T(\text{fit})\} \times 100]/\Delta^\circ H_T(\text{exp})$

$$C_P^{\text{Ti-Ta-Nb}} = x_{\text{Ti}} C_P^{\text{Ti}} + x_{\text{Ta}} C_P^{\text{Ta}} + x_{\text{Nb}} C_P^{\text{Nb}} \tag{12}$$

where x_{Ti}, $x_{\text{Ta,}}$ and x_{Nb} are mole fractions of Ti, Ta, and Nb in the alloy and C_P^{Ti}, C_P^{Ta}, and, C_P^{Nb} are specific heat values of Ti, Ta, and Nb, respectively. The input data for C_P of pure elements are taken from a standard source [24]. In Fig. 5, the N–K estimate is also co-plotted with the experimental data and it is readily observed that the estimated C_P is slightly higher than the experimental one; nevertheless, its behavior is quite similar to the experimental trend.

5 Conclusions

(1) An accurate determination of the temperature dependence of the enthalpy increment for Ti–5 mass% Ta–1.8 mass% Nb has been made in the temperature range from 463 K to 1457 K using inverse drop calorimetry. The measured data are subject to standard analytical treatment to obtain specific heat values for α- and β-phases.

(2) The drop calorimetry study clearly attested to the occurrence of the $\alpha \rightarrow \beta$ phase transformation in the temperature range from 1072 K to 1156 K. This temperature interval for the $\alpha \rightarrow \beta$ phase transformation has also been confirmed by microstructural studies.

(3) The $\alpha \rightarrow \beta$ phase transformation kinetics is assumed to follow the KJMA description of a diffusion-limited reaction. The apparent activation energy for the overall phase change is estimated to be 295 kJ · mol^{-1}.

(4) The latent heat associated with the phase transformation or the transformation enthalpy is estimated to be 76 J · g^{-1}. The corresponding change in specific heat $\Delta^\circ C_P$ is estimated as 904 J · kg^{-1} · K^{-1}.

(5) The measured specific heat values for the α phase are reasonably approximated by the Neumann–Kopp rule.

Table 5 Estimated specific-heat (C_P) data of Ti–5 mass% Ta–1.8 mass% Nb alloy using Eqs. 4 and 11 for α- and β- phases, respectively

Temperature (K)	C_P ($J \cdot kg^{-1} \cdot K^{-1}$)
α-Phase	
298	520
464	524
489	527
514	531
539	535
563	539
586	543
638	552
662	556
663	556
686	561
712	566
737	571
761	575
786	580
811	585
836	590
860	595
885	601
910	606
935	611
959	616
985	621
1009	626
1059	637
1072	640
1084	642
β-Phase	
1180	529
1180	529
1195	534
1205	538
1223	545
1230	547
1254	557
1258	558
1274	564
1280	566
1304	575

Table 5 continued

Temperature (K)	C_P ($J \cdot kg^{-1} \cdot K^{-1}$)
1329	584
1344	589
1357	594
1382	603
1407	612
1432	620
1432	620
1457	629

Acknowledgments The authors sincerely acknowledge Dr. Baldev Raj, Director, IGCAR, Dr. T. Jayakumar, Director, Metallurgy and Materials Group, and Dr. M. Vijayalakshmi Head, Physical Metallurgy Division for their sustained interest and encouragement. Mrs. Josephine Prabha is acknowledged for her assistance. Madhusmita Behera wishes to acknowledge DAE for the award of a Senior Research Fellowship, as a part of which this research is carried out.

Appendix

Estimation of β-phase Fraction Using ImageJ® Software

The β-phase fraction has been quantified by image analysis using the ImageJ® program. For this purpose, the SEM back scattered electron images obtained at different magnifications are used. Due to the partitioning of β stabilizing elements between the α- and β-phases, it is possible to use the mass contrast in the backscattered mode to distinguish between β (white) and α (black) coexisting phases with a scanning electron microscope. Image analysis has been performed on as-collected images using the threshold option in ImageJ®. The threshold limit is set in such a manner that the processed image resembled and matched quite well with the unprocessed original image, as shown in Fig. 6a, b. The quantification thus obtained is certainly subject to the limitations of image threshold setting parameters, and this is a difficult issue to

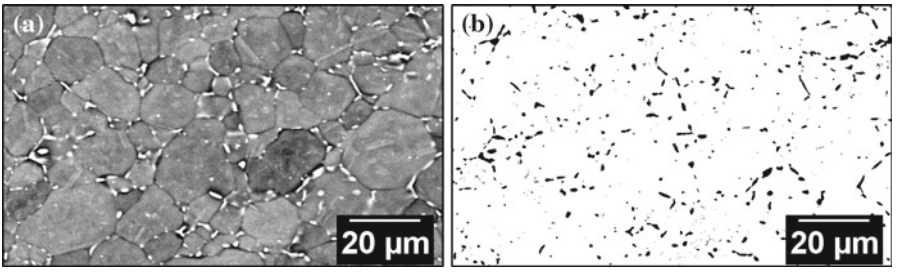

Fig. 6 (a) SEM backscattered image of 1073 K drop sample and (b) processed image using ImageJ® software, with threshold set for capturing the β-phase with a fair degree of resemblance to unprocessed image

quantify very objectively. In the case of the binary Ti–25.5 mass% Nb alloy that has been equilibrated for long time periods, we adopted a similar procedure to quantify the β-phase fraction against the standard values quoted by other studies and also obtained from an equilibrium diagram using the lever rule [25]. The relative merit of adopting an image analysis procedure for phase fraction quantification is calibrated from the results of this study. But it must be admitted that pending rigorous quantification using multi-cross sectional images and also a comparative study using X-ray profile analysis, where this method is applicable, the simple method adopted in the present study will be of use only in comparing the relative changes in the β-phase fraction as a function of temperature. Thus, the β-phase fraction in the sample that is dropped from 1060 K by the above procedure is estimated as $(3.73 \pm 0.5)\,\%$ with the remaining fraction of the microstructure attributed to the α-phase. A similar procedure has been followed to calculate the β-phase fraction of the sample dropped at 1083 K and the estimated β-phase fraction is $(6.56 \pm 1.3)\,\%$. In image analysis procedures, the uncertainty figure has no absolute meaning. However, we have performed the analysis on 12 different images obtained at the same and different magnifications, and also from different locations. The standard deviation of the volume fraction obtained is quoted as a typical uncertainty.

References

1. I.J. Polmear, *Light Alloys: From Traditional Alloys to Nano Crystals*, 4th edn. (Elsevier, Amsterdam, The Netherlands, 2006), p. 299
2. J.R. Davis, *Alloying: Understanding the Basics* (ASM International, Materials Park, OH, 2001), p. 417
3. T. Karthikeyan, R. Mythili, S. Saroja, M. Vijayalakshmi, Met. Mater. Process. **18**, 269 (2006)
4. S. Saroja, M. Vijayalakshmi, B. Raj, Trans. Indian Inst. Met. **61**, 389 (2008)
5. R. Mythili, S. Saroja, M. Vijayalakshmi, V.S. Raghunathan, J. Nucl. Mater. **345**, 167 (2005)
6. R. Mythili, A. Ravi Shankar, S. Saroja, V.R. Raju, M. Vijayalakshmi, R.K. Dayal, V.S. Raghunathan, R. Balasubramaniam, J. Mater. Sci. **42**, 5924 (2007)
7. R. Mythili, S. Saroja, M. Vijayalakshmi, Mater. Sci. Eng. A **454–455**, 43 (2007)
8. T. Karthikeyan, A. Dasgupta, S. Saroja, R. Khatirkar, M. Vijayalakshmi, I. Samajdar, Mater. Sci. Eng. A **485**, 581 (2008)
9. A. Banerjee, S. Raju, R. Divakar, E. Mohandas, Mater. Lett. **59**, 1219 (2005)
10. D.G. Archer, J. Phys. Chem. Ref. Data **22**, 1441 (1993)
11. R. Mythili, V. Thomas Paul, S. Saroja, M. Vijayalakshmi, V.S. Raghunathan, Mater. Sci. Eng. A **390**, 299 (2005)
12. P. Villars, J.L.C. Daams, J. Alloys Compd. **197**, 177 (1993)
13. S. Malinov, W. Sha, Z. Guo, C.C. Tang, A.E. Long, Mater. Charact. **48**, 279 (2002)
14. V. Anbarasan, B. Jeyaganesh, S. Raju, S. Murugesan, E. Mohandas, U. Kamachi Mudali, G. Manivasagam, J. Alloys Compd. **463**, 160 (2008)
15. R. Davis, H.M. Flower, D.R.F. West, J. Mater. Sci. **14**, 712 (1979)
16. Yu.K. Favstov, Met. Sci. Heat Treat. **40**, 29 (1998)
17. A.J. Prabha, S. Raju, B. Jeyaganesh, A.K. Rai, I. Johnson, in *Proceedings of the 17th National Symposium on Thermal Analysis (THERMANS-2010)*, ed. by P.C. Kalsi, R.V. Pai, M.R. Pai, S.R. Bharadwaj, V. Venugopal (SIRD, BARC, India, 2010), p. 42
18. H. Bros, M.L. Michel, R. Castanet, J. Therm. Anal. **41**, 7 (1994)
19. S. Raju, B. Jeyaganesh, A. Banerjee, E. Mohandas, Mater. Sci. Eng. A **465**, 29 (2007)
20. F. Liu, F. Sommer, E.J. Mittemeijer, Int. Mater. Rev. **52**, 193 (2007)
21. M.J. Starink, J. Mater. Sci. **32**, 6505 (1997)
22. G. Ruteinberg, E. Woldt, A.K. Petford-Long, Thermochim. Acta **378**, 97 (2001)

23. G. Grimvall, *Thermophysical Properties of Materials* (North-Holland, Amsterdam, Oxford, New York, Tokyo, 1986), p. 146
24. M.W. Chase, C.A. Davis, J.R. Downey, J. Frurip, R.A. McDonald, A.N. Syverud, *JANAF Thermochemical Tables*, 3rd edn. J. Phys. Chem. Ref. Data **14,** 1601, 1811, 1819, 1820 (1985)
25. J. Prabha, S. Raju, B. Jeyaganesh, A.K. Rai, M. Behera, M. Vijayalakshmi, G. Panneerselvam, I. Johnson, Philos. Mag. (submitted) (2010)